Forming a Ferrimagnetic-Like Structure in the $PbMn_{1-x}Fe_xBO_4$ ($x \approx 0.1$) Single Crystal upon Partial Substitution

A. Pankrats[1,2], M. Kolkov[1,2], A. Balaev[1], A. Shabanov[1], and A. Vasiliev[1,2]

[1]Kirensky Institute of Physics, Federal Research Center KSC SB RAS, Krasnoyarsk, 660036 Russia
[2]Siberian Federal University, Krasnoyarsk, 660041 Russia

Abstract—The $PbMn_{1-x}Fe_xBO_4$ ($x \approx 0.1$) orthoborate single crystals have been grown for the first time by spontaneous crystallization and their magnetic and resonance properties and specific heat have been examined. It has been established that partial substitution of iron ions for manganese ones leads to an increase in the Curie temperature to 34.2 K from its value of 30.3 K in the unsubstituted crystal, enhances the magnetic anisotropy, and reduces the saturation magnetization. The magnetization drop is explained in the framework of the model of a ferrimagnetic-like structure, in which the magnetic moments of iron and manganese ions form ferromagnetic sublattices coupled by the antiferromagnetic exchange.

It has been found that under magnetization along the rhombic ***b*** axis the magnetic moments switch stepwise to the magnetic field direction in a certain critical field. The spin-reorientation transition is the first-order one. This feature of the crystal magnetization does not allow the experimental ferromagnetic resonance frequency-field dependence to be described using the calculation for a simple rhombic ferromagnet. It has been established that the increase in the magnetic anisotropy of the crystal upon substitution leads to an increase in the energy gap in the ferromagnetic resonance spectrum to 121.5 GHz at T=4.2 K.

1. Introduction

The priority problems of physics of condensed matter are the search for new magnetic materials, their synthesis, and investigations. The researches in this field are aimed, on one hand, at designing novel functional materials for engineering applications and, on the other hand, at establishing new experimental facts, which stimulate a study of new physical phenomena at the intersection of magnetic, electrical, elastic, and other properties of solids.

Recently, there has been a keen interest in the Pb-bearing orthoborate crystal family with the general formula $PbABO_4$. The crystal structure of these materials at A = Ga, Al was investigated first by H. Park et al. [1], who established the orthorhombic structure with sp. gr. *Pnma*. The main structural elements of these crystals are chains of edge-sharing oxygen octahedra with A^{3+} ions at the center. The magnetic properties of the $PbABO_4$ (A = Fe, Cr, and Mn) crystals in the polycrystalline state were examined by the same team in [2]. It was found that the magnetic order type depends on the paramagnetic A ion. It was stated that the $PbABO_4$ (A = Fe, Cr) crystals are antiferromagnets with Neel temperatures of 125 and 8.3 K, respectively. The $PbABO_4$ (A = Mn) compound was the only in this row that possesses the ferromagnetic order.

Studies on single crystals yield much more reliable data, since polycrystalline objects can contain foreign crystal phases. We grew $PbFeBO_4$ single crystals by spontaneous crystallization using a flux technique and demonstrated [2] that the magnetic properties of single crystals are strongly different from those of polycrystals. The refined Neel temperature was found to be 115 K and the temperature dependence of the magnetic susceptibility corresponds to the three-dimensional magnetic structure model rather than to the quasi-one-dimensional model following form the polycrystal data [2]. In addition, we observed magnetodielectric anomalies in the $PbFeBO_4$ magnetic ordering region, which are indicative of the interplay between the magnetic and dielectric subsystems in a crystal.

Another advantage of the studies on single crystals is the possibility of investigations of the anisotropic properties of compounds. A study of the magnetic and resonance properties of the

$PbMnBO_4$ single crystals grown by us for the first time [4] showed that, below the Curie temperature T_C = 30.3 K, this compound is a strongly anisotropic ferromagnet. We believe that the static Jahn–Teller effect causes the formation of both the ferromagnetic exchange coupling in the MnO_6 octahedra chains and the strong magnetic anisotropy of the crystal. The considerable effective anisotropy fields in $PbMnBO_4$ determine an extremely large energy gap in the ferromagnetic resonance (FMR) spectrum, which attains 112 GHz at T= 4.2 K. In addition, it was found [5] that upon crystal heating in zero magnetic field a noticeable magnetic contribution to the specific heat is retained up to temperatures twice as high as the T_C value; in strong fields, this range becomes even broader. This fact, together with the strong difference between T_C and the paramagnetic Curie temperature θ = 49 K were attributed to the effect of a quasi-one-dimensional magnetic structure of the $PbMnBO_4$ crystal. The estimations showed that the difference between the parameters of ferromagnetic exchange interaction inside chains and between them is not as large as in ordinary quasi-one-dimensional magnets; for this reason, the temperature range of the short-range magnetic ordering is located in the paramagnetic region fairly close to T_C and increases the temperature range of existence of the magnetic contribution to the specific heat. This is the difference between the $PbMnBO_4$ crystal and both three-dimensional ferromagnets with the isotropic exchange coupling and conventional quasi-one-dimensional magnets, in which the correlations of the short-range magnetic order lead to the occurrence of a pronounced specific heat maximum in the paramagnetic temperature range fairly far from the magnetic phase transition temperature.

The partial or complete substitution of one ion for another in a crystal is often used in materials science for governing the magnetic properties of a crystal. This technique is especially effective in the compounds where the use of different paramagnetic ions in one crystallographic site makes it possible to synthesize a family of isomorphic crystals. For this purpose, 3d transition-metal ions or 4f rare-earth (RE) ions are most frequently used as paramagnetic ions; the most well-known examples of such isomorphic families are ferrites with a spinel [6] and garnet structures [7]. A great diversity of properties is typical of a RE orthoferrite and orthochromite $REFe(Cr)O_3$ family, in which, as in the garnet family, the substitution can be implemented in both the RE ion (including yttrium) and 3d ion subsystem. In orthoferrites, the replacement of one RE ion by another from the Y, Sm, Er, Dy, and Ho series strongly changes the magnetic anisotropy and resonance properties, as well as the magnetic phase diagram and a sequence of spin-reorientation transitions ([8–11]).

In recent years, the families of isomorphic crystals with the magnetic properties changing after the change of paramagnetic ions were found. A great number of works have been devoted to the magnetic and magnetoelectric properties of the $REFe_3(BO_3)_4$ RE crystals with a huntite structure. In these crystals, as in orthoferrites, the RE-ion subsystem is paramagnetic and polarized due to the exchange coupling with the iron subsystem. As a result, the RE subsystem significantly contributes to the magnetic anisotropic properties of the crystals and makes it possible to obtain a wide spectrum of antiferromagnetic structures, from simple easy-plane and easy-axis to noncollinear, including helical magnetic structures. In addition, this family is characterized by a strong dependence of the magnetoelectric [12] and magnetic resonance properties [13] on the RE ions used. Upon partial substitution of one RE ion for another or under diamagnetic dilution of the RE subsystem, the magnetic phase diagrams and other properties of the RE ferroborates also strongly change [14, 15].

Of even greater interest are the families of isomorphic crystals in which the replacement of one paramagnetic ion by another changes the magnetic order type. Examples of this fairly rare family are pyroxenes, including the $NaCrGe_2O_6$ chain ferromagnet [16] and $NaFeGe_2O_6$ multiferroic compound with a complex magnetic phase diagram containing incommensurately modulated antiferromagnetic structure of cycloidal type and sinusoidal spin-density wave configuration [17-20]. A great variety of magnetic structures is typical of the perovskite family, which involves the $BiMnO_3$ and $BiCrO_3$ solid solutions [21] with the well-studied magnetic properties; the former has a ferromagnetic structure and the latter is an antiferromagnet. The magnetic phase diagram of the $BiMn_{1-x}Cr_xO_3$ family contains, along with the initial ferro- and antiferromagnetic states, the ferrimagnetic-like state in the Mn-rich region of substitution and the spin-glass state at x=0.3–0.7.

We may assume that the intermixing of Mn^{3+} and Fe^{3+} ions in the magnetic subsystem of the $PbABO_4$ crystal will also lead to the formation of a more complex magnetic structure, since these ions in the $PbMnBO_4$ and $PbFeBO_4$ precursor crystals induce the exchange interactions with the opposite signs. To establish a trend in the magnetic structure variation, it is sufficient to begin the investigation with the relatively weak partial substitution of Fe^{3+} ions for Mn^{3+} ones. Therefore, the aim of this study was to investigate the magnetic, thermodynamic, and resonance properties of the $PbMn_{1-x}Fe_xBO_4$ ($x \approx 0.1$) single crystal.

In the course of thorough investigations of the specific heat and magnetization, we established a minor increase in the Curie temperature and a decrease in the saturation magnetization as compared with the values for the initial $PbMnBO_4$ crystal. The magnetization drop was explained using a model of the ferrimagnetic-like structure, in which the Mn^{3+} and Fe^{3+} ion subsystems from two ferromagnetic sublattices coupled by the antiferromagnetic exchange. A spin-reorientation transition under magnetization along the orthorhombic ***b*** axis was observed, which is most likely the first-order one. Due to this feature of magnetization along the ***b*** axis, the experimental FMR frequency-field dependence for this direction is poorly described by a theoretical dependence calculated for a simple rhombic ferromagnet.

2. Experimental details

The $PbMn_{1-x}Fe_xBO_4$ ($x \approx 0.1$) single crystals were grown first by spontaneous crystallization using a pseudo-flux technique. This technique was used to obtain the $PbMnBO_4$ and $PbFeBO_4$ single crystals [3, 4]. The feature of this technique is that the oxides contained in a solvent are included in the chemical composition of the synthesized compound. This approach excludes contamination of the crystal with foreign impurities. The solvent used was a well-known $PbO–B_2O_3$ system with an eutectic point of 768°C; however, taking into account the hygroscopicity of boron oxide, the final weight was added with 30% of this component. A platinum crucible with the $PbO–Mn_2O_3–Fe_2O_3–B_2O_3$ oxide mixture was heated in a vertical furnace to 1020 °C and, after exposure at this temperature for 3 h, cooled to 750 °C at a rate of 3.6 °C/h. The obtained black prismatic single crystals with a metallic luster were mechanically withdrawn from the crucible. The maximum sizes of the single crystals were $4 \times 1.0 \times 0.5$ mm^3. The X-ray diffraction analysis on a SMART APEX II single-crystal X-ray diffractometer confirmed the orthorhombic crystal structure (sp. gr. *Pnma*) with unit cell parameters of a = 6.77 Å, b = 5.94 Å, and c = 8.58 Å, which are similar to the parameters of the $PbMnBO_4$ single crystal [4]. The X-ray diffraction analysis confirmed also the high quality of the single crystals and showed the ab-

sence of twinning and foreign phase impurities. Similar to the unsubstituted compound, the single-crystal face with the maximum area is the (101) crystallographic plane and the maximum crystal size coincides with the orthorhombic ***b*** axis.

The real iron content in the crystals was determined by the X-ray fluorescence analysis on a Hitachi Tabletop Microscope TM3000. To exclude the effect of contaminations and defect states on the natural faces, the analysis of the content was performed on the fresh-cleaved single-crystal surface; the spot type was 5-10 μm. The similar analysis was carried out for a few crystals taken from the same crucible from which samples were selected for all measurements. We found a slight spread of the iron content between individual single crystals and in the bulk of

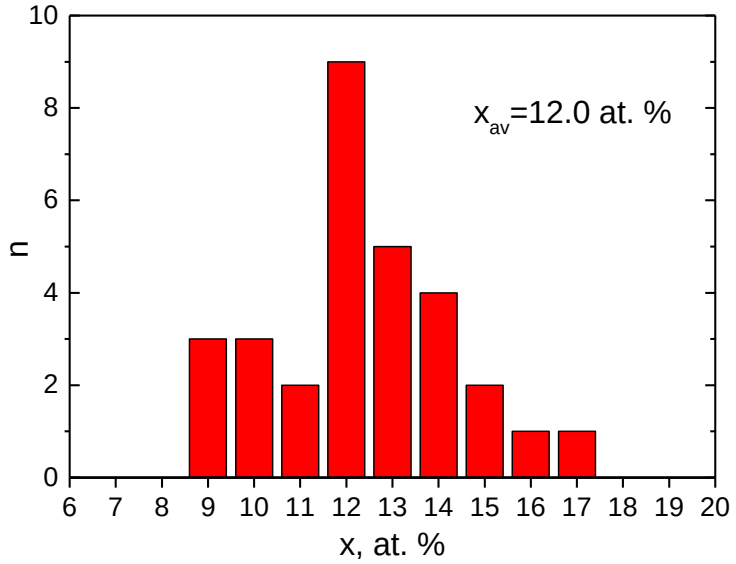

Fig. 1. Histogram of the real Fe content distribution in the $PbMn_{1-x}Fe_xBO_4$ single crystal.

them. Fig.1 shows a histogram of the local iron content distribution over the cleavage surface of one of the single crystals. Other cleavage surfaces of the same single crystal show a close distribution of local iron content. The iron ion content averaged over all the measurements for this single crystal is 12.0 at. %, which is somewhat higher than the iron content in a charge. The average iron content in different single crystals lies between 8–15 at. %.

The magnetization of the $PbMn_{1-x}Fe_xBO_4$ single crystals was measured using a conventional vibrating sample magnetometer (VSM) with a superconducting solenoid operating in the temperature range of 4.2–300 K and magnetic fields up to 70kOe [22]. To measure specific heat at temperatures of 2–300 K in magnetic fields, a Quantum Design PPMS-9 Physical Property Measurement System was used.

The FMR study of the $PbMn_{0.9}Fe_{0.1}BO_4$ single crystals was carried out on an original magnetic resonance spectrometer with the broad (25–130 GHz) frequency band in pulsed magnetic fields up to 90 kOe [23].

3. Results and discussion

3.1. Magnetic properties

The static magnetic properties of the $PbMn_{0.9}Fe_{0.1}BO_4$ single crystals were studied on a vibrating sample magnetometer with a superconducting solenoid in wide field and temperature ranges. A prismatic sample was glued on a triangular quartz prism, which allowed us to easily connect to the three rhombic directions. Temperature dependences of the magnetic susceptibility for the $PbMn_{1-x}Fe_xBO_4$ single crystal measured along the rhombic crystal axes in a magnetic field of 1 kOe (Fig. 2a) are similar to the dependences for the unsubstituted $PbMnBO_4$ crystal

[4]. The Curie temperature T_c = 35.5 K determined from the maximum derivative dχ/dT at the **H**||***a*** orientation is somewhat higher than the Curie temperature T_c = 30.3 K in the unsubstituted

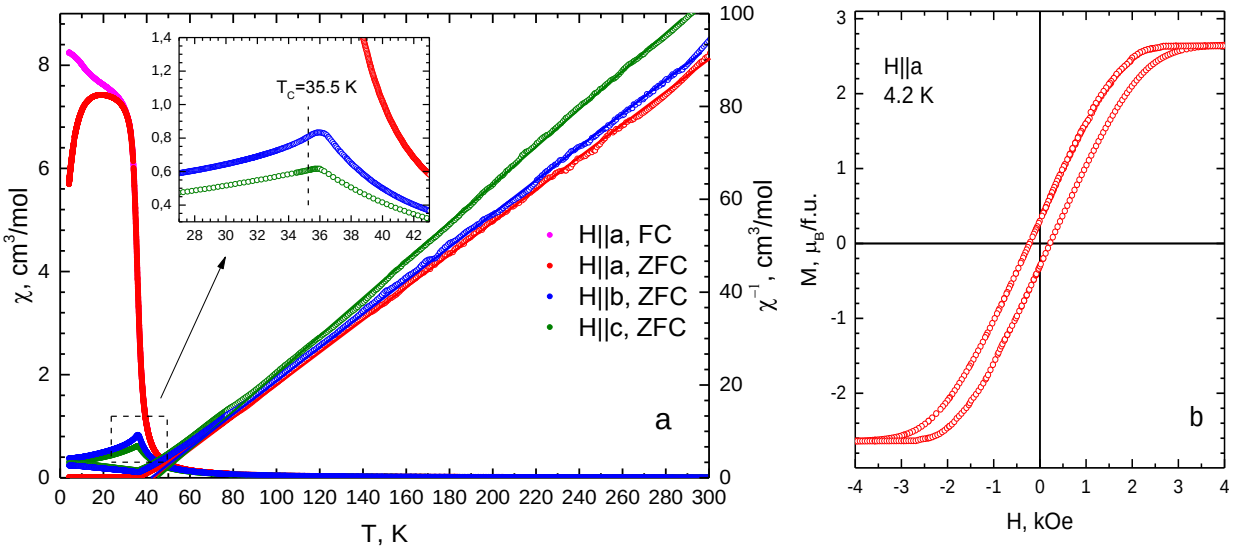

Fig. 2. a - temperature dependences of the magnetic susceptibility and reciprocal susceptibility measured along all the orthorhombic axes in a magnetic field of 1 kOe; insert: fragment of the temperature dependences of the magnetic susceptibility near the Curie temperature. b - hysteresis loop measured at T=4.2 K along the ***a*** axis

$PbMnBO_4$ crystal. Similar to the unsubstituted crystal, $PbMn_{1-x}Fe_xBO_4$ is characterized by the strong anisotropy of the magnetic properties in the ordered temperature region. At low temperatures, the $M(T)$ dependences at **H**||***a*** behave differently upon cooling in a magnetic field and without field, which is caused by the domain structure formation. As in the unsubstituted crystal, the temperature dependences of magnetization in the ***b*** and ***c*** rhombic axes directions have sharp maxima in the vicinity of a magnetic phase transition, which show that both directions are hard magnetization axes [4].

In the paramagnetic region, the temperature dependences of the reciprocal magnetic susceptibility also demonstrate a noticeable magnetic anisotropy. Using the Curie–Weiss approximation of the temperature dependences of the reciprocal susceptibility $\chi^{-1}(T)$ in the temperature range of T >100 K for the three rhombic directions, we calculated the paramagnetic Curie temperatures θ_a = 43 K, θ_b=42 K, and θ_c= 45 K and the effective magnetic moments μ_a= 4.75 μ_B, μ_b= 4.71 μ_B, and μ_c = 4.45 μ_B. It is worth noting that the difference between T_c and paramagnetic Curie temperatures in the substituted crystal is somewhat smaller than in the unsubstituted crystal. This fact most likely indicates that upon iron ion substitution the difference between the exchange interactions inside chains and between them becomes smaller than in the unsubstituted crystal [5]. This is consistent with the Curie temperature growth upon substitution due to an increase in the exchange coupling between chains.

The hysteresis loop measured at T=4.2 K in the magnetic field directed along the ***a*** axis (see Fig. 3) indicates the presence of a spontaneous magnetic moment. Note that the coercive field H_c=220 Oe of Fe-doped crystal increased in comparison with H_c=50 Oe of unsubstituted one [4].

The field dependences of magnetization measured along the three rhombic directions also show a pronounced magnetic anisotropy (Fig.3). These dependences confirm that, as in the unsubstituted crystal, the easy magnetization axis coincides with the rhombic ***a*** direction.

Note that the saturation magnetization determined from the high-field portion of the dependence for **H**||**a** is M_s = 2.67 μ_B/f.u. at T=4.2 K, which is significantly lower than ~4 μ_B/f.u. in the unsubstituted sample. Such a magnetization drop can be explained in the framework of a model of the ferrimagnetic-like structure, where the Mn^{3+} and Fe^{3+} ions form two antiferromagnetically coupled sublattices. A similar model was used to explain the magnetic phase diagram of the $BiMn_{1-x}Cr_xO_3$ solid solutions [21]. In this case, the saturation magnetization per formula unit is determined by the equation

$$M_s = M_{Mn} \cdot (1-x) - M_{Fe} \cdot x \quad , \qquad (1)$$

where $M_{Mn} = 4\ \mu_B$ and $M_{Fe} = 5\ \mu_B$ are the magnetic moments of Mn^{3+} and Fe^{3+} ions, respectively, and x is the substitution coefficient. Using a value of M_s = 2.67 μ_B/f.u. at T=4.2 K, we obtain a substitution coefficient of x = 0.148. This is consistent with the X-ray fluorescence data.

The field dependences of magnetization measured along the rhombic ***b*** axis at temperatures below T_c (Fig. 3b) have a specific shape, which is especially pronounced below 20 K. In the initial portion, the magnetization increases monotonically and almost linearly with the field; then, at approaching certain critical field H_c, the magnetization increases stepwise to saturation. The inset in Fig. 4 shows an enlarged fragment of the field dependence of magnetization at T=4.2 K. The pronounced hysteresis of the dependence in the measurements with increasing and decreasing field suggests that this step is a first-order spin-reorientation transition. The temperature dependence of the transition critical field H_c, which is determined as a field corresponding to the middle of the jump, is presented in Fig. 4.

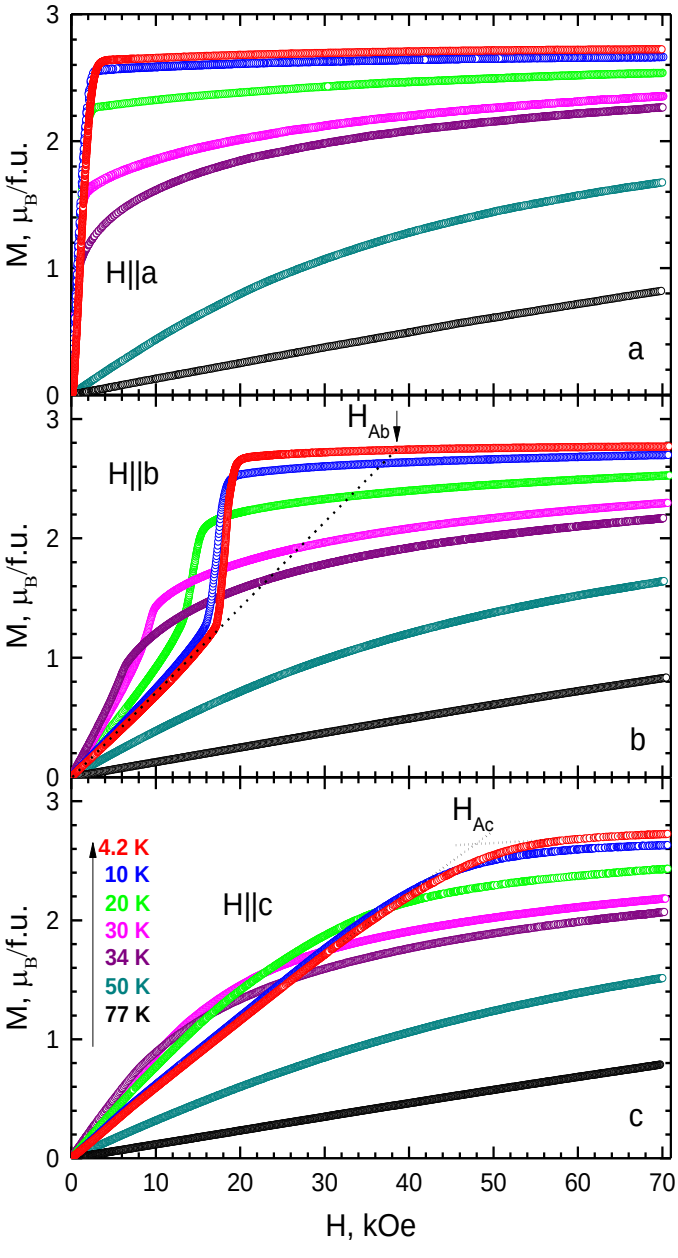

Fig. 3. Field dependences of the magnetization measured along three orthorhombic axes.

According to the field dependences of magnetization for $PbMnBO_4$ [4], the magnetization of the unsubstituted crystal at the same field direction also saturates stepwise. However, this transition in the unsubstituted crystal is weaker than in the substituted one and can be clearly observed only below 10 K. Physically, this spin-reorientation transition apparently originates from the features

of the magnetic structure of this crystal family. As we mentioned in [4], the strong magnetic anisotropy of this crystal results from the Jahn–Teller distortions of oxygen octahedra surrounding Mn^{3+} ions. The feature of the magnetic structure of both pure and partially substituted $PbMnBO_4$ crystals is that the macroscopic magnetic anisotropy is characterized by an easy magnetization axis, which coincides with the rhombic ***a*** axis and two other rhombic ***b*** and ***c*** axes are hard. At the same time, the crystal structure contains four types of the local anisotropy axes with the directions strongly different from the orientations of the averaged macroscopic axes. In particular, the local anisotropy axes of neighboring ions in a chain extended along the ***b*** axis make an angle of ~83.4° with each other (Fig. 12 in [4]). In addition, the local anisotropy planes in the exchange-coupled neighboring chains are symmetrically rotated relative to the ***ac*** plane by angles of ±28°. The strong magnetic anisotropy of the Mn^{3+} ion and such a complex pattern of the local anisotropy axes most likely lead to the spin-reorientation transition accompanying the magnetization along the chain (***b*** axis). Theoretical calculations [24] confirm this scenario.

Under magnetization along the rhombic ***c*** axis, the field dependences of magnetization (Fig. 3c) are similar to the dependences in unsubstituted $PbMnBO_4$. In the ordered temperature region, the magnetization linearly increases with the field almost up to saturation; the saturation fields H_{Ac} were defined as fields of intersection of the straights approximating the linear portions of the dependences before and after saturation (dotted lines in Fig. 3c). The temperature dependence of the saturation field H_{Ac} is shown in Fig. 4.

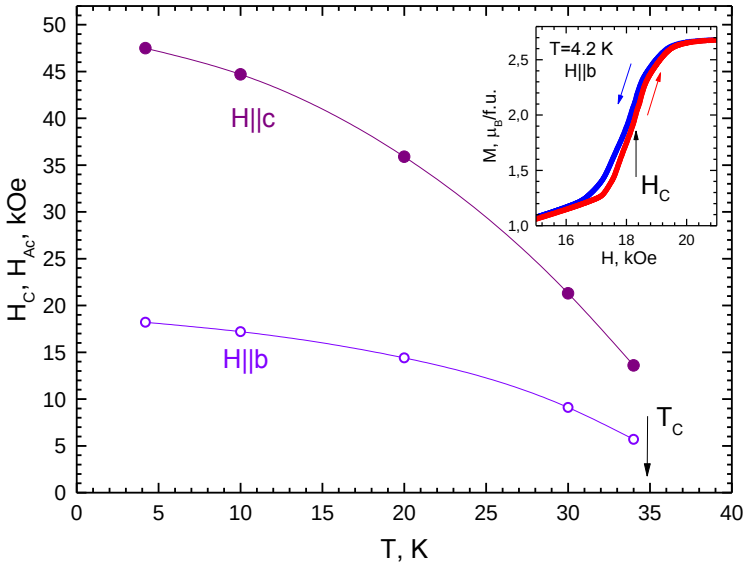

Fig. 4. Temperature dependences of the critical field H_c at H||b and saturation magnetization field H_{Ac} at H||c. Inset: hysteresis of the field dependence of the magnetization upon spin reorientation at H||b. T = 4.2 K.

In the paramagnetic temperature region, the field dependences of magnetization for all the rhombic directions remain nonlinear up to nitrogen temperatures.

3.2. Specific Heat

The temperature dependence of specific heat of the $PbMn_{1-x}Fe_xBO_4$ crystal measured in zero magnetic field is presented in Fig. 5 (closed circles). For comparison, the temperature dependence of specific heat (open circles) at $H = 0$ for the unsubstituted $PbMnBO_4$ crystal from [5] is shown. The pronounced λ–peak of the specific heat indicates that the improved Curie temperature T_c =34.2 K slightly increased as compared with its value in the unsubstituted crystal. As in the $PbMnBO_4$ crystal, the specific heat peak is smeared in a magnetic field of $H = 3$ kOe.

In addition, Fig. 5 shows the lattice contribution to the specific heat of the $PbMnBO_4$ crys-

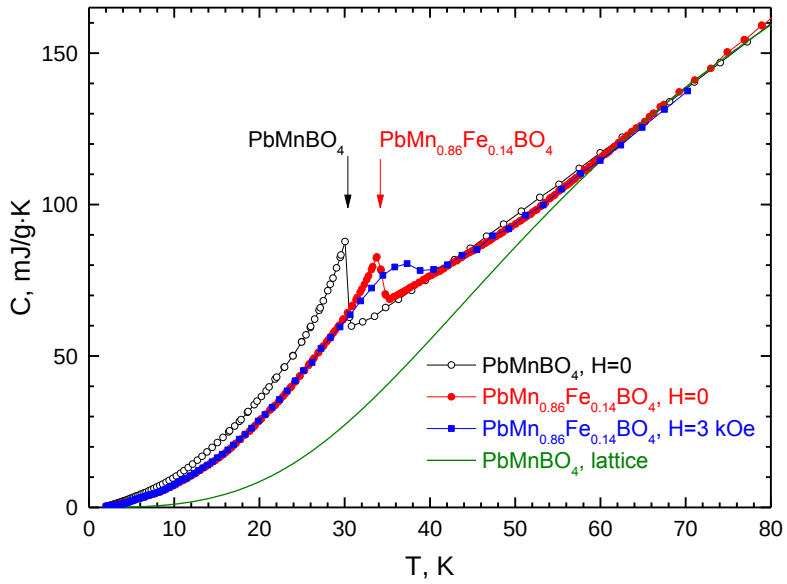

Fig. 5. Temperature dependences of specific heat of the $PbMn_{1-x}Fe_xBO_4$ crystal measured at H=0 (closed circles) and 3 kOe (squares) and $PbMnBO_4$ crystal measured at H = 0 (open circles). The solid line shows the lattice contribution calculated for $PbMnBO_4$.

tal calculated using the Debye–Einstein model (solid line) [4]. The experimental specific heat of the $PbMn_{1-x}Fe_xBO_4$ crystal can be presented as a sum of the magnetic and lattice contributions. The temperature dependence of the magnetic contribution to the specific heat at $H = 0$ is presented in Fig. 6. The comparison with the temperature dependence of the magnetic contribution for unsubstituted $PbMnBO_4$ (dotted line) shows that in the substituted crystal the magnetic contribution in the paramagnetic region also remains in a fairly wide temperature range above T_c. This fact together with the above-mentioned nonlinearity of the field dependences of magnetization in the paramagnetic region show that the quasi-one-dimensional magnetic structure of the $PbMnBO_4$ crystal [5] does not change upon substitution. Nevertheless, the tail of the magnetic contribution to the specific heat in the substituted $PbMn_{1-x}Fe_xBO_4$ crystal decreases a bit faster than in the unsubstituted one. Therefore, we may assume that upon iron ion substitution the difference between the exchange couplings inside chains and between them becomes smaller than in pure $PbMnBO_4$. This assumption seems quite reasonable, taking into account that the difference between the Curie temperature T_c and paramagnetic Curie temperature θ also noticeably decreased upon substitution.

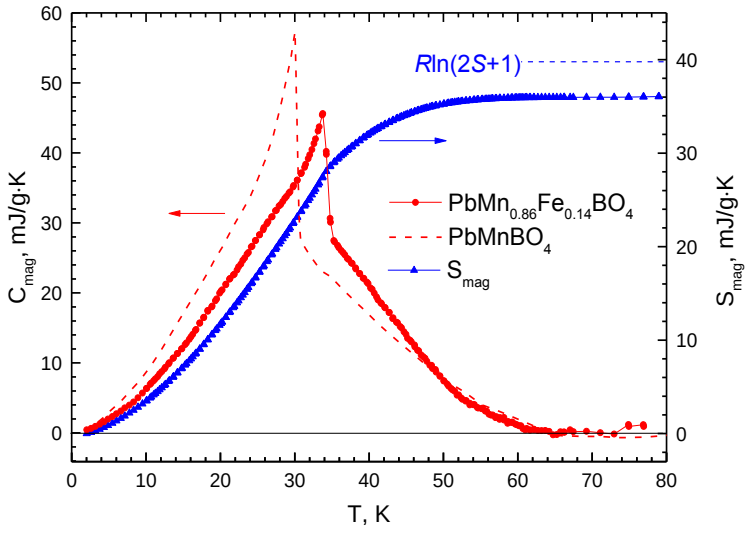

Fig. 6. Temperature dependences of the magnetic contributions to the specific heat of the $PbMn_{1-x}Fe_xBO_4$ (red circles) and $PbMnBO_4$ crystals (dotted line) and magnetic entropy of the $PbMn_{1-x}Fe_xBO_4$ crystals (blue triangles) at H = 0.

The temperature dependence of the magnetic contribution to the specific heat allows us to calculate the magnetic contribution to the transition entropy; the temperature dependence of the

latter is also presented in Fig. 6. As in pure $PbMnBO_4$, the transition entropy in zero magnetic field attains saturation, which is similar to the quantity $R\ln(2S+1)$ typical of the magnetic transitions at a temperature of ~55 K far above the T_c value. This also evidences for the effect of a quasi-one-dimensional magnetic structure on the magnetic transition in the $PbMn_{1-x}Fe_xBO_4$ crystal, as it occurs in pure $PbMnBO_4$ [5].

3.3. Ferromagnetic resonance

The magnetic resonance in the $PbMn_{1-x}Fe_xBO_4$ crystals was investigated at T=4.2 K in the frequency range of 30–125 GHz at the two magnetic field orientations, **H**||***b*** and **H**||***c***. The measurements were performed on a parallelepiped sample with the long axis coinciding with the orthorhombic ***b*** axis; the directions of the other axes were determined by the X-ray diffraction analysis. The FMR frequency-field dependence in a magnetic field applied along the orthorhombic ***c*** axis is presented in Fig. 7a. The dependence has a form typical of the field orientation in the hard direction. The dependence is characterized by softening of the resonance frequency in the region of the anisotropy field for this direction. The experimental data are described well by the theoretical dependences obtained for a rhombic ferromagnet [25]:

$$H < H_{Ac}, \quad \nu = \gamma\sqrt{H_{Ab}H_{Ac} - \frac{H^2 H_{Ab}}{H_{Ac}}}, \qquad (2)$$

$$H > H_{Ac}, \quad \nu = \gamma\sqrt{H + \left(H_{Ab} - H_{Ac}\right)} \cdot \sqrt{H - H_{Ac}}.$$

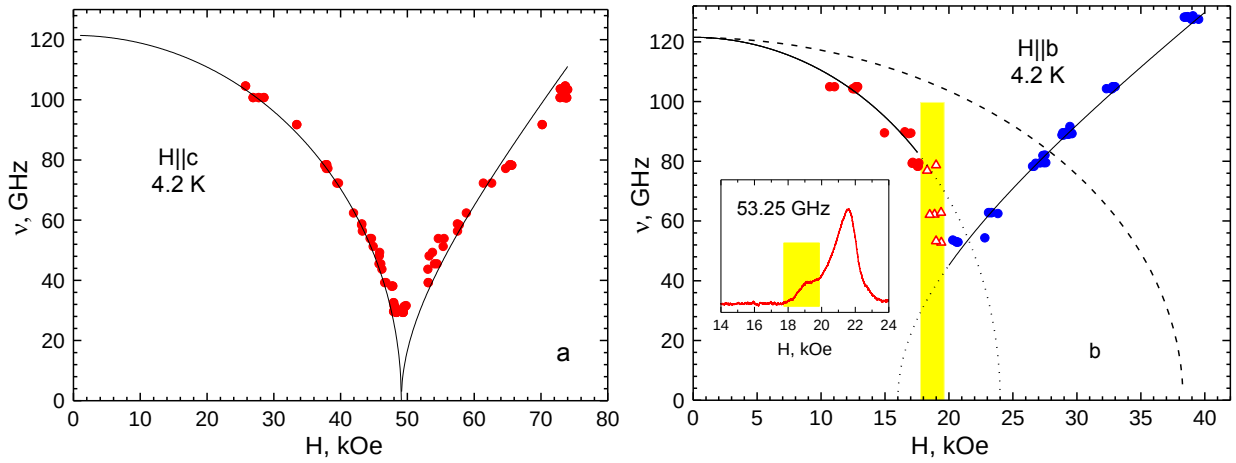

Fig.7. Frequency-field dependences of the FMR in $PbMn_{1-x}Fe_xBO_4$ at T = 4.2 K and different magnetic field orientations: (a) H||c and (b) H||b. Inset: resonance spectrum fragment for H||b at a frequency of 53.25 GHz. The yellow bands in Fig. 7b and the inset indicate the field range of the spin-reorientation transition.

Here, γ is the gyromagnetic ratio and H_{Ab} and H_{Ac} are the magnetic anisotropy fields for the ***b*** and ***c*** directions, respectively. Solid lines show the theoretical dependences built using fitting parameters given in Table 1. The determined anisotropy field H_{Ac} coincides with the saturation field obtained from the field dependence of magnetization at this orientation (see Fig. 3c) at T=4.2 K. The anisotropy field H_{Ab} is similar to the saturation field obtained at the intersection of

the saturation magnetization level with the dotted line that continues the initial linear portion of the field dependence (see Fig. 3b). For a temperature of T=4.2 K, this field is shown by the arrow in Fig. 3b; it is the saturation field value that would be observed at this orientation in the absence of the spin-reorientation transition.

The energy gap in the FMR spectrum at T=4.2 K is ν_c = 121.5 GHz. A certain increase in this gap as compared with a value of 112 GHz in the unsubstituted crystal is caused by the enhancement of the magnetic anisotropy upon substitution, which is confirmed also by a minor increase in the saturation fields in the field dependences of magnetization (Figs. 3b, 3c) as compared with the case of the unsubstituted crystal. At first sight, the anisotropy growth upon partial substitution of Fe^{3+} ions for the strongly anisotropic Mn^{3+} ions is unexpected. Although we failed to find a spin-flop transition in $PbFeBO_4$ [3] and estimate the anisotropy field for this crystal, it is clear from the general considerations that the anisotropic properties of the Fe^{3+}ion are much weaker than the anisotropy of the Mn^{3+} ion. Therefore, it would be reasonable to expect a decrease in the magnetic anisotropy upon substitution; the experiment, however, demonstrates the opposite situation. In the substituted crystal, oxygen octahedra surrounding the neighboring Mn^{3+} and Fe^{3+} ions apparently experience additional distortions as compared with their sites in the unsubstituted $PbMnBO_4$ and $PbFeBO_4$ crystals, which leads to the enhancement of the anisotropic properties upon partial substitution.

It is worth noting that the resonance properties of the substituted and unsubstituted crystals at the **H**||***c*** orientation are very similar, except for the above-mentioned difference between energy gaps in the FMR spectra. At the **H**||***b*** orientation, however, the difference between the frequency-field properties of the crystals is greater (Fig. 7b). In contrast to $PbMnBO_4$, the resonance frequency softening in the substituted crystal does not occur up to zero frequency and the resonance absorption in the anisotropy field range at this orientation is not observed below~50 GHz. This is apparently due to the fact that under magnetization of the crystal in this direction, the magnetic moments smoothly rotate in the magnetic field direction only to a certain critical field, in which they rotate stepwise in the ***b*** axis direction. The magnetic field range of the spin-reorientation transition is highlighted in yellow in Fig. 7b. In this region, one can observe the features related to the change in the reflection from a short-circuited waveguide with a sample upon variation in the crystal magnetic state during the spin-reorientation transition. The inset in Fig. 7b shows a fragment of the resonance absorption spectrum at a frequency of 53.25 GHz, where the spin-reorientation region highlighted in yellow includes the signal variation under reorientation of the magnetic moments. Since these features are observed in this field range at different frequencies, they represent a non-resonance response. The experimental points corresponding to the non-resonance response are shown by triangles in the frequency-field dependence.

The description of the FMR frequency-field dependences at **H**||***b*** using formulas (2) with the replacement $H_{Ac} \leftrightarrow H_{Ab}$ [25] only makes sense beyond the reorientation region. The attempt of such a description with the parameters obtained for the case **H**||***c*** appeared unsuccessful. The dotted line in Fig. 7 shows the theoretical dependence calculated for the descending FMR branch in the range of $H<H_{Ab}$ = 38.3 kOe with the specified set of parameters. This dependence is essentially different from the experimental one. The experimental data for this direction can be formally described using dependences (2) for the set of parameters in which the H_{Ac} value is the same as in the ***c*** axis direction and the γ and H_{Ab} values are different. This sets of parameters are given in Table 1. Solid lines in Fig. 7b show frequency-field dependences calculated for these

sets of parameters in magnetic fields before and after the spin-reorientation transition. It can be seen that the magnetic fields corresponding to the resonance frequency softening are significantly weaker than 38.3 kOe. The descending FMR branch corresponds to $H_{Ab}>H_c$ and the ascending branch, to $H_{Ab}<H_c$, which is characteristic of a first-order phase transition with the overlap of the regions of existence of the states before and after the transition. For the same reason, the FMR frequency does not soften to zero in the spin reorientation region.

Table 1

Parameters γ, H_{Ab}, and H_{Ac} fitted from FMR

Field orientation and range	γ, MHz/Oe	H_{Ab}, kOe	H_{Ac}, kOe
$\mathbf{H}\|\|\boldsymbol{c}$, $H< H_{Ac}$, $H> H_{Ac}$	2.80±0.02	38.3± 0.4	49.1±0,3
$\mathbf{H}\|\|\boldsymbol{b}$, $H< H_c$	3.5 ±0.1	24.0 ± 0.5	49.1±0,3
$\mathbf{H}\|\|\boldsymbol{b}$, $H>H_c$	3.1 ±0.1	16.0 ± 0.5	49.1±0,3

Thus, the variety of the magnetic properties of the $PbMn_{1-x}Fe_xBO_4$ crystal under magnetization along the orthorhombic ***b*** axis prevents the adequate description of the FMR frequency-field dependence for this direction using the theoretical dependences for a simple ferromagnet with the orthorhombic symmetry.

Concerning the comparison of the resonance properties of the $PbMn_{1-x}Fe_xBO_4$ and $PbMnBO_4$ crystals, we would like to emphasize the following. For the unsubstituted $PbMnBO_4$ crystal, we managed to describe the resonance properties for all the three orthorhombic directions by one set of parameters: γ = 3.4 MHz/Oe, H_{Ab} = 22.6 kOe, and H_{Ac}= 47.5kOe. The comparison of this set with the field dependences of the magnetization for $PbMnBO_4$ at T = 4.2 K shows that only the anisotropy field H_{Ac} used in describing the resonance properties coincides with the saturation field at H||c, while the anisotropy field H_{Ab} used is intermediate between an experimental saturation field of 20 kOe (this is, in fact, the field of a spin-reorientation transition in the unsubstituted crystal) and a saturation field of ~35 kOe, which corresponds to the initial linear portion of the field dependence of magnetization at $\mathbf{H}\|\boldsymbol{b}$. In this case, the gyromagnetic ratio γ exceeds by far a reasonable value of 2.8 MHz/Oe. Thus, although the spin-reorientation transition in the unsubstituted $PbMnBO_4$ crystal is weaker than in the substituted one, it, however, significantly affects the description of the resonance properties of the crystal.

In the easy direction (at $\mathbf{H}\|\boldsymbol{a}$), the FMR resonance frequency grows almost linearly with an increase in a magnetic field [25]. At such an orientation of the magnetic field, we could not observe the FMR in the $PbMn_{1-x}Fe_xBO_4$ crystal because the gap in the FMR spectrum is close to the upper limit of the spectrometer working frequencies.

4. Conclusions

The $PbMn_{1-x}Fe_xBO_4$ ($x \approx 0.1$) orthoborate single crystals were grown for the first time by spontaneous crystallization and their magnetic and resonance properties and specific heat were investigated.

It was found that the partial iron ion substitution led to an increase in the Curie temperature to 34.2 K from a value of 30.3 K in the unsubstituted crystal. The growth of the Curie tempera-

ture upon substitution over the value for pure manganese orthoborate can be attributed to the enhancement of the exchange coupling between chains by iron ions.

In addition, it was established that the substitution induced an increase in the magnetic anisotropy and a decrease in the saturation magnetization. The magnetization drop was explained using a model of the ferrimagnetic-like structure, in which the magnetic moments of iron and manganese ions form ferromagnetic sublattices coupled by the antiferromagnetic exchange.

It was observed that under magnetization along the rhombic ***b*** axis at a certain critical field the magnetic moments switch stepwise to the magnetic field direction. The spin-reorientation transition is first-order. It is most likely caused by the strong magnetic anisotropy of the Mn^{3+} ion and features of the crystal structure, which contains four types of the local anisotropy axes making different angles with the averaged macroscopic anisotropy axes of the crystal.

The study of the resonance properties showed that the enhancement of the magnetic anisotropy upon substitution increased the energy gap in the FMR spectrum to ν_c = 121.5 GHz at T = 4.2 K from a value of 112 GHz in the unsubstituted crystal.

The theoretical frequency-field dependences calculated for a simple rhombic ferromagnet describe well the experimental dependences measured along the ***c*** axis. However, this approach cannot adequately describe the similar dependence for the ***b*** axis because of the complex magnetic structure transformation under magnetization in this direction.

Acknowledgments

The authors are grateful to S. Nikitin for help in the specific heat measurements in a magnetic field and S. Martynov for fruitful discussions.

This study was funded by RFBR and the Government of Krasnoyarsk Territory, Krasnoyarsk Regional Fund of Science, to the research project no. 18-42-240008 "Effect of Magnetic Structure on the Magnetodielectric Properties of Oxide Crystals Containing Stereoactive Ions Pb^{2+} and Bi^{3+}".

References

[1] H. Park and J. Barbier, *Acta Crystallogr*. E57 (2001) 82.
[2] H. Park, R. Lam, J.E. Greedan and J. Barbier, *Chem. Mater.* 15 (2003) 1703.
[3] A. Pankrats, K. Sablina, D. Velikanov, A. Vorotynov, O. Bayukov, A. Eremin, M. Molokeev, S. Popkov and A. Krasikov, *JMMM* 353 (2014) 23.
[4] A. Pankrats, K. Sablina, M. Eremin, A. Balaev, M. Kolkov, V. Tugarinov and A. Bovina, *JMMM* 414 (2016) 82.
[5] A. Pankrats, M. Kolkov, S. Martynov, S. Popkov, A. Krasikov, A. Balaev, M. Gorev, *JMMM* 471 (2019) 416.
[6] J. Smit, H.P.J. Wijn, Ferrites, John Wiley and Sons, New York, 1959.
[7] A.H. Morrish, The physical principles of magnetism, John Wiley and Sons, NewYork, 1965.
[8] K.P. Belov, A.K. Zvezdin, A.M. Kadomtseva, R.Z. Levitin, Orientational Transitions in Rare-Earth Magnets, Nauka, 1979.
[9] V. I. Ozhogin, V. G. Shapiro, K. G. Gurtovoi, E. A. Galst'yan, A. Ya. Chervonenkis, *JETP* 35 (1972) 1162.

[10] K.B. Aring, A.J. Sievers, *J. Appl. Phys.* 41 (1970) 1197.
[11] A. M. Balbashov, A. A. Volkov, S. P. Lebedev, A. A. Mukhin, A. S. Prokhorov, *JETP* 61 (1985) 573.
[12] A.M. Kadomtseva, Yu.F. Popov, G.P. Vorob'ev, A.P. Pyatakov, S.S. Krotov, K.I. Kamilov, V.Yu. Ivanov, A.A. Mukhin, A.K. Zvezdin, A.M. Kuz'menko, L.N. Bezmaternykh, I.A. Gudim and V.L. Temerov, *Low Temperature Physics* 36 (2010) 511.
[13] A.M. Kuz'menko, A.A. Mukhin, V.Yu. Ivanov, A.M. Kadomtseva, S.P. Lebedev, and L.N. Bezmaternykh, *JETP* 113 (2011) 113.
[14] M. Platunov, N. Kazak, V. Dudnikov, V. Temerov, I. Gudim, Yu. Knyazev, S. Gavrilkin, V. Dyadkin, Iu. Dovgaliuk, D. Chernyshov, A. Hen, F. Wilhelm, A. Rogalev, and S. Ovchinnikov, *JMMM* 479 (2019) 312.
[15] C. Ritter, A.I. Pankrats, A.A. Demidov, D.A. Velikanov, V.L. Temerov, and I.A. Gudim, *Phys. Rev. B* 91 (2015) 134416.
[16] G. Nénert, C. Ritter, M. Isobe, O. Isnard, A.N. Vasiliev, and Y. Ueda, *Phys. Rev. B* 80 (2009) 024402.
[17] G. J. Redhammer, A. Senyshyn, M. Meven, G. Roth, S. Prinz, A. Pachler, G. Tippelt, C. Pietzonka, W. Treutmann, M. Hoelzel, B. Pedersen, G. Amthauer, *Phys. Chem. Minerals* 38 (2011) 139.
[18] T.V. Drokina, G.A. Petrakovskii, L. Keller, J. Schefer, A.D. Balaev, A.V. Kartashev, D.A. Ivanov, *JETP* 112 (2011) 121.
[19] L. Ding, P. Manuel, D. Khalyavin, F. Orlandi, and A. Tsirlin, *Phys. Rev. B* 98 (2018) 094416.
[20] Ingyu Kim, Byung-Gu Jeon, D. Patil, S. Patil, G. Nénert and Kee Hoon Kim, *J. Phys.: Condens. Matter* 24 (2012) 306001.
[21] A.A. Belik, *Inorganic Chemistry* 55 (2016) 12348.
[22] A.D. Balaev, Yu.V. Boyarshinov, M.M. Karpenko, B.P. Khrustalev, *Prib. Tekh. Eksp.* 3 (1985) 167.
[23] V.I.Tugarinov, I.Ya. Makievskii, A.I.Pankrats, *Instrum. Exp. Tech.* 47 (2004) 472.
[24] S. Martynov, *JETP* (2020) in press.
[25] A.I. Pankrats, V.I. Tugarinov, K.A. Sablina, *JMMM* 279 (2004) 231.